Proceedings of the 3rd International Congress APMAS2013, April 24–28, 2013, Antalya, Turkey

Growth Analysis and Numerical Simulation of Cu_3BiS_3 Absorbing Layer Solar Cell through the wxAMPS and Finite Element Method

F. Mesa[a,*], V. Ballesteros[a] and A. Dussan[b]

[a]Departamento de Ciencias Básicas, Universidad Libre, Cra. 70 N° 53-40, Bogota, Colombia

[b]Departamento de Fisica, Universidad Nacional de Colombia, Cra. 30 N° 45-03, Bogota, Colombia

The properties and the efficiency of a semiconductor thin film depend on the state of stress and defects in the film structure. When the film is growing layer by layer, the elastic energy due to deformation stress between the substrate and the film is released partly due to the formation of dislocations in the critical thickness deformation. In this paper, we present a finite element analysis of the stress state in a thin film of Cu_3BiS_3 as a function of thickness and elastic energy release by nucleation of dislocations. Initially, we analyze the stress contours associated with the epitaxial growth and dislocation nucleation and then combine these two in order to study the effective potential energy state of the system. Finally, the tool wxAMPS is today an important application for simulation of solar cells with high reliability and an improved design over its analysis of microelectronic and photonic structures predecessor, incorporating physical principles concerning photovoltaic phenomena and uses a new method for solving algorithms, combining Newton and Gummel approaches, which provides greater stability and speed of computation.

DOI: 10.12693/APhysPolA.125.385

PACS: 68.35.Rh, 02.70.Bf, 07.05.Tp, 68.55.ag

1. Introduction

The properties and efficiency of heteroepitaxial semiconductor thin films depend upon states of stress and defects in the film structure. Recent years, it has carried out an extensive work as for characterization of thin films, with special emphasis on the nucleation and the generation of dislocations [1, 2].

During the epitaxial growth, the first layers are fully consistent with the matrix with tetragonal distortion of the film lattice. Whether, the film has a higher lattice parameter, then the film is under compression while the substrate under tension. Initially, for the first layers, the elastic energy stored in the film is not suitable for nuclear dislocation, but as the film thickness increases then begins nucleation of dislocations and thus, the thickness in which this occurs is designated as critical thickness (h_c). General, there are three approaches to determine the critical thickness at which nucleation starts dislocations:

I. Minimization of the total addition energies of deformation due to film growth and dislocation energy [3].

II. Matching the strain energy with the dislocation energy [4].

III. Assumption that the film has excess stress and is in a metastable state [5].

2. Dislocation energy

Elastically stored energy in a coherent isotropic film parallel to crystallographic plane (0 0 1), (1 1 1) or (0 1 1) is given by

$$E_h = 2Gf_m^2 h\left(\frac{1+v}{1-v}\right), \quad (1)$$

where f_m is the strain rate of the lattice, h is the film thickness, G and v correspond to the shear modulus and Poisson's ratio, respectively, of thin film material, E_h is the strain energy per unit area of the sample. Edge dislocation decreases the maximum strain rate, which is proportional to the Burgers vector $\boldsymbol{b}$, while a pure helical dislocation does not contribute to this reduction. The energy per unit length of an edge dislocation, such as that obtained from the theory of elasticity, using a Volterra cut is given by [6]:

$$E_{\rm dl} = \frac{Gb^2}{4\pi(1-v)}\left[2+\ln\left(\frac{\gamma_0}{b}\right)\right], \quad (2)$$

where γ_0 represents the size of the control volume and is taken such as $70\boldsymbol{b}$ approximate and $E_{\rm dl}$ is the energy per unit length of the dislocation line. The total energy in the thin film in presence of dislocations is

$$E_{\rm total} = E_h + E_{\rm dl}. \quad (3)$$

It is noted that E_h has units of energy per unit area and $E_{\rm dl}$ is expressed in units of energy per unit length, this implies that $E_{\rm dl}$ should be normalized with a length and may make corresponding operation with E_h.

Carrying out a division by using this length and $\gamma_0 = h$ can be successfully established $E_{\rm total}$ that is a function of the thickness of the thin film. This is emphasized that this length has been chosen by some authors as the Burgers vector [7]. Since the core radius is often greater than this length, it would be more appropriate to consider a distance from the power supply which dislocation formation, this length is taken such as $5\boldsymbol{b}$ [4]. This value is approximately equal to the lateral expansion of the area under tension [8].

*corresponding author; e-mail: fgmesar@unal.edu.co

3. Finite element analysis

3.1. Coherent of thin film growth

It is expected that the linear relationship of E_h with h is true for any thin film (Eq. (1)) [9]. As the growth proceeds, the upper layers will be of more relaxed energy than the layers closest to the substrate [10], although there is no evidence geometric relaxation. Consequently, the energy per unit area of the sample should increase with the thickness, but presents a significant decrease [11].

3.2. Simulation of the nucleation of a strain dislocation

To carry out the simulation, we propose a rectangular domain of 200 Å × 150 Å, discretized with a mesh of 50×50 quadrangular finite elements of standard type [12]. Figure 1 shows the location of the dislocations, where are presented with two states at different times for a configuration of sources 30 and 900 planes, showing the displacement and annihilation of dislocations and the deformation of the mesh.

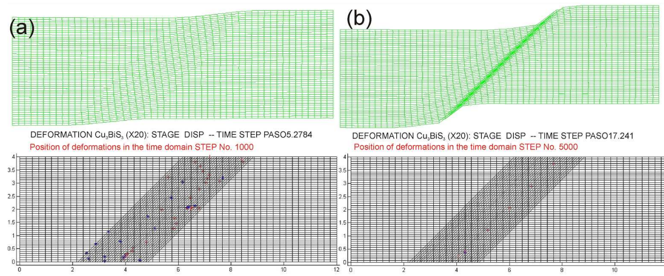

Fig. 1. Location of dislocations in step (a) 1000 and (b) 5000. The deformation of the mesh with 30 planes and 900 strains is displayed.

4. Results and discussion

4.1. Critical thickness

The equilibrium theory of Frank and Van der Merve [3] takes into consideration only the energy in the sample. Using this magnitude in the finite element simulation [13], it is possible to determine the critical thickness of the thin film proposed for analysis. To accomplish this purpose it is convenient to effect a diagram that represents the energy per unit area at the interface both before and after introduction of a dislocation in the system [14].

By reference to the graph shown in Fig. 2, at distances of $\boldsymbol{b}/2$ and $5\boldsymbol{b}/2$ energy per unit area is between about 0.56 and 0.02 J/m^2, respectively. The thickness, in that the stored energy in the film tensioned by unit area of the interface, exceeds the threshold limits corresponding to two critical values that can be termed as peaks and correspond to the critical thickness [15]. For the case of a thin film of Cu_3BiS_3, through the finite element method is a $6\boldsymbol{b}$ critical thickness. Additionally, it is expected that the level of metastability of the film depends on the configuration of the same, either metallic or semiconductor, which at the same time determines the extent of dislocation nucleation and density dislocations existing.

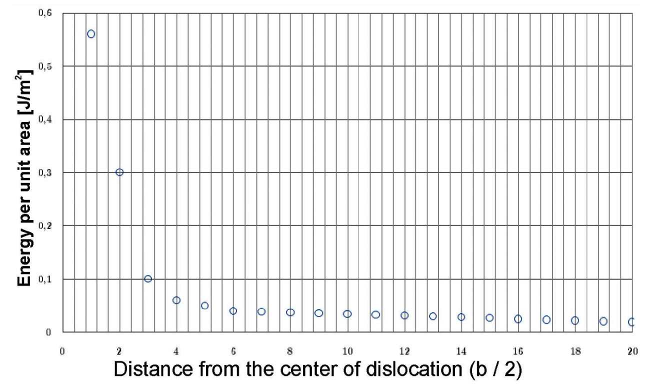

Fig. 2. Variation of energy per unit area (film–substrate interface).

4.2. Current–voltage characteristic

This feature could play a significant part in the semiconductor solar cells [16], due to the low toxicity of bismuth compared with of $CuInGaSe_2$ (CIGS), the ternary Cu_3BiS_3 constitutes a favorable option for the development of new materials applied photovoltaic devices. Finally, the tool wxAMPS is today an important application for simulating solar cells with high reliability and improved design over its analysis of microelectronic and photonic structures (AMPS) predecessor [17], which incorporates physical principles concerning photovoltaic phenomena and uses a new method algorithms for solving combining Newton and Gummel approaches, which provides greater stability and computing speed.

However, in this work we used a computer PowerEdge T320 with Intel ® Xeon ® processor, 8 GB RDIMM, 500 GB 7.2 k RPM HD, OS Red Hat Enterprise Linux (RHEL 6.0), the Linux version of the wxAMPS free software distributed from the University of Illinois and the Linux version of the SCAPS software. On the other hand, the numerical simulation was attended with known photovoltaic parameters in order to estimate unknown quantities and associated diagrams.

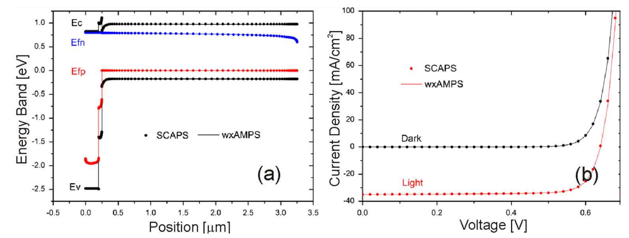

Fig. 3. Bands diagram (a) and I–V characteristic (b) of solar cells based on the Cu_3BiS_3 compound.

Figure 3 shows the diagrams obtained with wxAMPS and SCAPS for the Cu_3BiS_3 absorber layer of solar cell. In Fig. 3a it can be seen the energy band diagram showing a bias voltage of 0.845 V under illumination, while the diagram of Fig. 3b shows the current–voltage curves in conditions dark/light.

In wxAMPS initial conditions predicted for solar cell of Cu_3BiS_3 compound that was used such as an absorbent layer, obtained a $V_{oc} = 0.712$ V, $J_{sc} = 36.25$ mA/cm^2, $FF = 79.54\%$, and an efficiency of 19.86%, which allows us to infer Cu_3BiS_3 that constitutes an outstanding alternative to the design of photovoltaic devices.

5. Conclusions

We used the finite element method to simulate the nucleation of dislocations of Cu_3BiS_3 thin film. Based on a previously defined model, simulated a helical dislocation and through the analysis of energy conditions there was obtained critical thickness value for the sample semiconductor 6***b***. Moreover, it is noted that large photovoltaic conversion efficiencies can occur, with a new material with properties similar to CIGS.

Acknowledgments

This work was supported by Universidad Libre and COLCIENCIAS.

References

[1] S.C. Jain, J.R. Willis, R. Bullough, *Adv. Phys.* **39**, 127 (1990).

[2] S.C. Jain, A.H. Harker, R.A. Cowley, *Philos. Mag. A* **75**, 1461 (1997).

[3] F.C. Frank, J. Van der Merve, *Proc. R. Soc. A* **198**, 216 (1949).

[4] R. People, J.C. Bean, *Appl. Phys. Lett.* **49**, 229 (1985).

[5] J.Y. Tsao, B.W. Dodson, S.T. Picraux, D.M. Cornelison, *Phys. Rev. Lett.* **59**, 2455 (1987).

[6] W. Bollmann, *Crystal Defects and Crystalline Interfaces*, Springer, Berlin 1970.

[7] C.W. Pei, B. Turk, W.I. Wang, T.S. Kuan, *J. Appl. Phys.* **90**, 5959 (2001).

[8] P.M.J. Maree, J.C. Barbour, J.F. Van der Veen, K.L. Kavanagh, C.W.T. Bulle-Lieuwma, M.P.A. Viegers, *J. Appl. Phys.* **62**, 4413 (1987).

[9] A. Bradley, *Optical Storage for Computers Technology and Applications*, Ellis Horwood Ltd, New York 1989.

[10] G.B. Sakr, I.S. Yahia, M. Fadel, S.S. Fouad, N. Romcevic, *J. Alloys Comp.* **507**, 557 (2010).

[11] J.C. Manifacier, J. Gasiot, J.P. Fillard, *J. Phys. E* **9**, 1002 (1976).

[12] J.P. Hirth, J. Lothe, *Theory of Dislocations*, McGraw-Hill, New York 1968.

[13] J.S. Sanghara, I.D. Agarwal, *J. Non-Cryst. Solids* **256**, 6 (1999).

[14] K. Schwartz, *The Physics of Optical Recording*, Springer-Verlag, Berlin 1993.

[15] J.P. Dismukes, L. Ekstrom, R.J. Paff, *J. Phys. Chem.* **68**, 3021 (1964).

[16] F. Mesa, G. Gordillo, Th. Dittrich, K. Ellmer, R. Baier, S. Sadewasser, *Appl. Phys. Lett.* **96**, 082113 (2010).

[17] H. Zhu, A.K. Kalkan, J. Hou, S.J. Fonash, in: *Proc. Nat. Center for Photovoltaics (NCPV), 15th Program Review Meeting, Denver (CO)*, 1999, p. 309.